




How Comets Work

M. Fulle¹ , J. Blum², and A. Rotundi³¹ INAF—Osservatorio Astronomico, Via Tiepolo 11, I-34143 Trieste, Italy; marco.fulle@inaf.it² Inst. für Geophysik und extraterrestrische Physik, Techn. Univ. Braunschweig, Mendelssohnstr. 3, D-38106 Braunschweig, Germany³ Università degli Studi di Napoli Parthenope, Dip. di Scienze e Tecnologie, CDN IC4, I-80143 Naples, Italy

Received 2019 May 3; revised 2019 June 11; accepted 2019 June 11; published 2019 July 1

Abstract

Two major questions regarding comets have been up to now far from any solution. (i) How is it possible that water-ice sublimation from the nucleus surface does not lead to an insulating crust, stopping every gas and dust ejection within a few days? (ii) How is it possible that the gas flow crossing the refractory surface crust ejects dust particles bonded by tensile strengths larger than tens of Pa when the perihelion gas pressure at the nucleus-coma interface is less than one Pa? We have developed a simple but rigorous analytical model, assuming that the cometary nucleus consists of agglomerates of ice and dust (“clusters”). As soon as the clusters become exposed to sunlight, gas diffusion from their inside leads to their dehydration. We find that (i) the gas diffusing from the interior to the surface of a sunlit cluster has a steep density gradient at the cluster surface, which blasts the cluster into particles of sizes larger than or equal to those actually observed by *Rosetta* dust instruments; (ii) the heat-conduction and diffusion timescales are much shorter than the dehydration timescale, ensuring that the described process prevents any dumping of the nucleus activity driven by water-ice sublimation from 4 au inbound to 4 au outbound; and (iii) the clusters are in fact cm-sized pebbles, so that a cometary nucleus made of pebbles is confirmed to be the only one consistent with cometary gas and dust activity, a process unexplained until now.

Key words: comets: general – comets: individual (67P/Churyumov–Gerasimenko) – space vehicles: instruments

1. Introduction

Although the *Rosetta* mission to comet 67P/Churyumov–Gerasimenko (67P hereafter) has provided plenty of data to constrain cometary models, the activity paradox (Blum et al. 2014) has been not explained up to now: (i) How is it possible that water-ice sublimation from the nucleus surface does not lead to an insulating crust, stopping every gas and dust ejection (Kührt & Keller 1994; Blum et al. 2014)? (ii) How is it possible that the gas, flowing through the nucleus surface with a pressure < 1 Pa at perihelion (Pajola et al. 2017), ejects dust particles whose tensile strengths are > 10 Pa (Skorov & Blum 2012; Gundlach et al. 2015; Güttler et al. 2019)? Here we show that the dehydration (Fulle et al. 2019) of the clusters of agglomerates of ice and dust (“clusters” hereafter) (Güttler et al. 2019) constituting the surface layer of a cometary nucleus uniquely provides a direct physically self-consistent solution to the two long-standing unsolved questions.

2. Clusters Dehydration

Here we assume that comet nuclei are composed of clusters of agglomerates (Güttler et al. 2019) with an average radius R . Agglomerates are porous particles composed of ice and dust grains (Güttler et al. 2019). According to all available data, the refractory-to-ice mass ratio in comets is ≥ 3 (Fulle et al. 2019). Therefore, we assume that the matrix of each particle is refractory, with water-ice uniformly distributed inside it, either in the form of ice grains, or in the form of ice shells embedding dust grains. During its orbit, 67P ejected dust larger than the depth of the sublimation front of water ice (Rotundi et al. 2015; Fulle et al. 2016b; Ott et al. 2017; Fulle et al. 2019). It follows that, after the ejection of the largest dust particles, clusters with their pristine content of water ice become suddenly sunlit, and start to dehydrate (Fulle et al. 2019).

The agglomerates are porous, similarly to interplanetary dust particles of cometary origin (Rietmeijer 1998; Levasseur-Regourd et al. 2018; Güttler et al. 2019), well described by random-packing theory, with a porosity close to 50% (Fulle et al. 2016a, 2017; Levasseur-Regourd et al. 2018; Güttler et al. 2019), and composed of grains (monomers) of average diameter of 100 nm (Bentley et al. 2016; Levasseur-Regourd et al. 2018; Güttler et al. 2019; Mannel et al. 2019). It follows that the gas sublimating off the water ice inside the particles can reach the cluster surface only through the voids among the monomer grains. The average radius a of such voids (or pores) is 20% of the monomer diameter (Fulle & Blum 2017), i.e., $a = 20$ nm (Table 1 contains a list of all physical parameters). The mean free path of the water molecules is (Crifo 1989)

$$L = \frac{16\mu}{5P} \sqrt{\frac{kT}{2\pi m}} \quad (1)$$

where $\mu \approx 5 \cdot 10^{-5}$ kg m⁻¹ s⁻¹ is the viscosity for water vapor at the temperature $200 < T < 300$ K (Crifo 1989), k is the Boltzmann constant, m is the mass of the water molecule, and $L > 1$ mm for $P < 20$ Pa. Thus, each water molecule will be reflected when it collides with a dust monomer until it reaches the cluster surface, crossing the pores along its trajectory without any inter-molecular collision. This is a typical process of diffusion and results in a gas number density that is much higher inside the cluster than outside, i.e., with a pressure gradient between the cluster interior and its environment.

Along the radial coordinate r from the cluster center $r = 0$ to the cluster radius $r = R$, the steady-state gas number density, ρ (units mol m⁻³), is linked to the gas flux by Fick’s first law (Satterfield 1970), which in spherical coordinates is

$$D \frac{d\rho}{dr} + q = 0 \quad (2)$$

Table 1
List of Symbols

Symbol	Physical Parameter	Units
R	Average radius of the clusters of agglomerates of ice and dust grains	m
r	Variable radius inside the clusters of agglomerates of ice and dust	m
a	Average radius of the pores among the dust grains	m
s	Size (diameter) of the dust particles ejected from the cluster surface	m
L	Mean free path of water molecules	m
μ	Viscosity for water vapor	kg m ⁻¹ s ⁻¹
P	Pressure of the water vapor inside the clusters of agglomerates	Pa
S	Tensile strength bonding the agglomerates inside the clusters	Pa
T	Temperature of the water vapor	K
k	Boltzmann constant	J K ⁻¹
m	Mass of a water molecule	kg
ρ	Gas number density	mol m ⁻³
q	Gas flux inside the clusters of agglomerates of ice and dust grains	mol m ⁻² s ⁻¹
Q	Average gas flux from the nucleus surface	mol m ⁻² s ⁻¹
D	Gas diffusivity inside the clusters of agglomerates of ice and dust	m ² s ⁻¹
ρ_d	Average density of the dust particles	kg m ⁻³
c_p	Heat capacity of the clusters of agglomerates of ice and dust	J kg ⁻¹ K ⁻¹
λ_s	Heat conductivity of the clusters of agglomerates of ice and dust	W m ⁻¹ K ⁻¹

where D is the diffusivity and q (units mol m⁻² s⁻¹) describes the gas flux from all the homogeneously distributed sources inside the cluster. When $L \gg a$, the diffusion occurs in the Knudsen regime (Knudsen 1928; Smith 1970)

$$D = \frac{4a}{3} \sqrt{\frac{2kT}{\pi m}}. \quad (3)$$

For $T = 250$ K and $a = 20$ nm, we get $D = 7.2 \cdot 10^{-6}$ m² s⁻¹. Laboratory experiments performed with diluted gases flowing through random-packed silica spheres of radius ranging from 10 to 100 nm have confirmed the D values computed by Equation (3) (Huizenga 1984). Following the assumption of water-ice sources uniformly distributed inside the cluster, we can compute q according to the uniform and isothermal distribution of the q -sources

$$dq = \frac{4\pi Q r^2 dr}{\frac{4}{3}\pi R^3}, \quad (4)$$

where Q is the gas flow from the nucleus, providing $q = Q(r/R)^3$. The straightforward integration of Equation (2) then provides a gas number density inside the cluster of

$$\rho = \rho_s + \frac{QR}{4D} [1 - (r/R)^4] \quad (5)$$

where ρ_s is the gas number density just outside of the cluster. Inside the cluster, the differential of the gas number density close to the cluster surface can be approximated to $\Delta\rho = Qs/D$, where $s = (R - r) \ll R$ is the distance from the cluster surface. Therefore, the differential of the pressure at the cluster surface is

$\Delta P = QskT/D$, i.e., using D in Equation (3)

$$\Delta P = \frac{3Qs}{4a} \sqrt{\frac{\pi}{2} mkT}. \quad (6)$$

Regarding the tensile strengths bonding the dust particles composing a cluster, we assume here that the cluster is not perfectly homogeneous, otherwise its internal tensile strength would be on the order of 10 kPa (Skorov & Blum 2012; Gundlach et al. 2018), which is not overcome by sublimating water ice at $T < 300$ K (Blum et al. 2017). Each cluster is an agglomerate of dust particles of randomly distributed diameters s (in meters) bonded by the tensile strength $S = 13 s^{-2/3}$ mPa for a filling factor of 0.5 (Skorov & Blum 2012; Gundlach et al. 2015). This scaling law has been confirmed by laboratory experiments (Blum et al. 2014; Brisset et al. 2016). Equation (6) is independent of R , providing the same differential of the pressure at the surfaces of all particles building up the cluster, because $s \gg a$. At perihelion, the thermophysical model of a pebble-made nucleus provided a dehydration rate of $Q = 3.3 \cdot 10^{20}$ mol m⁻² s⁻¹ (Fulle et al. 2019), i.e., $T \approx 250$ K (Blum et al. 2017), so that Equation (6) provides $\Delta P \geq S$ for $s \geq 50 \mu\text{m}$ ($\Delta P \leq 10$ Pa). Excluded outbursts (which cannot be explained by the here-proposed continuous process), there is no evidence that 67P ever ejected particles with $s < 50 \mu\text{m}$ (Bentley et al. 2016; Moreno et al. 2017; Lévassieur-Regourd et al. 2018; Güttler et al. 2019). On 2014 August, Hapi's surface temperature was $T \approx 230$ K (Tosi et al. 2019), with Q values that are a factor ≈ 10 lower than at perihelion (Blum et al. 2017), providing $\Delta P \geq S$ when $s \geq 0.2$ mm. On 2014 August–September, only one dust particle crossing the Grain Impact Analyser and Dust Accumulator Grain Detection System (GIADA-GDS; Rotundi et al. 2015) was slightly smaller than such a size. During the same period, all the particles collected by the COmetary Secondary Ion Mass Analyser (COSIMA) were consistent with fragments (due to impacts on the instrument funnel) of dust parents larger than 0.2 mm (Schulz et al. 2015).

3. Diffusion, Heat-conduction, and Dehydration Timescales

Rosetta data provided the 67P dust size distribution from sub-micron to meter sizes (Rotundi et al. 2015; Bentley et al. 2016; Fulle et al. 2016b; Ott et al. 2017; Lévassieur-Regourd et al. 2018; Güttler et al. 2019), with a volume distribution that is dominated by the largest particles up to $R \approx 0.2$ m (Pajola et al. 2017; Fulle et al. 2019). Therefore, the diffusion timescale is on the order of $R^2/D \geq 0.5$ hr (Carr 2017) for $R \geq 0.1$ m. Because the 67P activity has never shown such a time delay at each sunrise, we can conclude that $R \ll 0.1$ m; i.e., that the clusters are in fact cm-sized pebbles (Blum et al. 2017).

The heat-conduction timescale is on the order of $4R^2 \rho_d c_p / \lambda_s \approx 2$ hr with $R \approx 5$ mm, $\rho_d \approx 800$ kg m⁻³ (Fulle et al. 2017), $c_p \approx 10^3$ J kg⁻¹ K⁻¹ (Blum et al. 2017) and $\lambda_s \approx 10^{-2}$ W m⁻¹ K⁻¹ (Arakawa et al. 2019), which is an order of magnitude shorter than the dehydration timescale, on the order of 2 days (Fulle et al. 2019). As it is exposed to sunlight, a pressure gradient inside the still non-isothermal pebble starts to erode it. After about 2 hr, the pebble has reached an almost uniform temperature, and Equation (6) precisely describes the gas density drop inside the pebble. These facts ensure us that the layer of dehydrating pebbles can always be eroded into dust before all the water ice inside the

sunlit pebbles is completely sublimated; i.e., that cometary activity may never stop, solving directly the abovementioned activity paradox (Kührt & Keller 1994; Blum et al. 2014).

At perihelion, the observed loss rate of sub-cm dust particles requires an erosion of about 1 cm over the dehydration timescale (Fulle et al. 2019), suggesting that dehydration may sometimes be faster than surface erosion. In order to make our steady model valid, the vertical erosion rate must range from 0.5 cm day^{-1} (dehydration-driven) to 12 cm day^{-1} (heat-conduction-driven). The dehydration rate Q computed by means of the thermophysical model of a pebble-made nucleus is independent of its refractory-to-ice mass ratio (Fulle et al. 2019), so that the proposed diffusion model explains also the ongoing cometary activity observed inbound from dust deposits composed of pebble-made dm-sized chunks (Pajola et al. 2017), probably characterized by ice mass fractions of very few% (Fulle et al. 2019).

4. Uniqueness of the Pebble Dehydration Model

The proposed dehydration and erosion model is self-sustaining and explains cometary activity with a macro-porosity having a scale length R close to 1 cm. The gas flux coming from below the surface pebble layer fills the macro-pores on a timescale that is orders of magnitude shorter than 1 s, with no pressure difference at the dust surface. In order to maintain a water gas flow crossing a cm-thick dehydrated dust layer (a thickness constrained by the 67P dust particles ejected from 2014 August to perihelion), it must have macro-pores of hundreds of microns (Hu et al. 2017) to not dump all water-ice sublimation, so that also in this case the dominating gas flux fills the macro-pores, with no pressure difference at the dust surface. A comet nucleus made of pebbles, thus having micro- and macro-porosities with typical scale lengths $a < 0.1 \mu\text{m}$ and $R < 0.1 \text{ m}$, respectively, may be the only one consistent with all available cometary and protoplanetary disk data (Blum et al. 2017). Pebbles are the main source of gas: the sublimation of ice grains external to pebbles cannot provide any pressure gradient able to blast the clusters of agglomerates into the observed dust particles.

5. Conclusions

To explain cometary activity, we developed a simple but rigorous analytical model of gas diffusion (Knudsen 1928) for a comet-nucleus structure that is consistent with all *Rosetta* data: made of pebbles, i.e., cm-sized agglomerates of ice and refractory particles (Blum et al. 2017). The model follows the diffusion of the gas through the pores of a sunlit pebble, from the inside to the outside, during its dehydration (Fulle et al. 2019). Gas diffusion naturally transforms sunlit pebbles into small “pressure cookers.” We find the following.

- (i) Inside the sunlit pebble, the water ice sublimates and the gas diffuses with a steep density drop at its surface, which breaks the pebble into dust particles of sizes larger than or equal to those actually observed during the entire *Rosetta* mission at 67P, if the pebbles are not homogeneous in tensile strength, following a scaling law (Skorov & Blum 2012).
- (ii) The heat-conduction and diffusion timescales are much shorter than the 67P erosion timescale observed at perihelion, ensuring that the described process feeds a nucleus activity driven by water-ice sublimation from 4 au inbound to 4 au outbound.
- (iii) A cometary nucleus made of pristine pebbles (Blum et al. 2017), i.e., the only one consistent with most 67P data, is

coherent with the above-listed conclusions, providing a frame that solves the activity paradox (Kührt & Keller 1994; Blum et al. 2014).

Our model explains the steady dust release driven by water-ice sublimation. It cannot explain outbursts (Vincent et al. 2016; Agarwal et al. 2017), possibly ejecting dust smaller than $50 \mu\text{m}$ (Bockelée-Morvan et al. 2017; Güttler et al. 2019), and the ejection of chunks bigger than pebbles (Fulle et al. 2016b, 2019; Ott et al. 2017), probably driven by the sublimation of supervolatiles.

We thank an anonymous referee for improving this Letter, and the *Rosetta* Science Ground Segment at ESAC, the *Rosetta* Mission Operations Centre at ESOC, and the *Rosetta* Project at ESTEC for their outstanding work enabling the science return of the *Rosetta* Mission. Part of this research was supported by the ESA Express Procurement (EXPRO) RFP for IPL-PSS/JD/190.2016 and by the Italian Space Agency (ASI) within the ASI-INAF agreements I/032/05/0 and I/024/12/0. J.B. thanks the Deutsche Forschungsgemeinschaft for support under grant BL298/26-1 as part of the international CoPhyLab collaboration. CoPhyLab is jointly funded through DFG (Germany), FWF (Austria), and SNF (Switzerland).

ORCID iDs

M. Fulle  <https://orcid.org/0000-0001-8435-5287>

References

- Agarwal, J., Della Corte, V., Feldman, P. D., et al. 2017, *MNRAS*, 469, S606
 Arakawa, S., Tatsuuma, M., Sakatani, N., & Nakamoto, T. 2019, *Icar*, 324, 8
 Bentley, M., Schmier, R., Mannel, T., et al. 2016, *Natur*, 537, 73
 Blum, J., Gundlach, B., Krause, M., et al. 2017, *MNRAS*, 469, S755
 Blum, J., Gundlach, B., Mühle, S., & Trigo-Rodrigues, J. M. 2014, *Icar*, 235, 156
 Bockelée-Morvan, D., Rinaldi, G., Erard, S., et al. 2017, *MNRAS*, 469, S443
 Brisset, J., Heisselmann, D., Kothe, S., Weidling, R., & Blum, J. 2016, *A&A*, 593, A3
 Carr, E. J. 2017, *PhRvE*, 96, 012116
 Crifo, J. F. 1989, *A&A*, 223, 365
 Fulle, M., & Blum, J. 2017, *MNRAS*, 469, S39
 Fulle, M., Blum, J., Green, S., et al. 2019, *MNRAS*, 482, 3326
 Fulle, M., Della Corte, V., Rotundi, A., et al. 2016a, *MNRAS*, 462, S132
 Fulle, M., Della Corte, V., Rotundi, A., et al. 2017, *MNRAS*, 469, S45
 Fulle, M., Marzari, F., Della Corte, V., et al. 2016b, *ApJ*, 821, 19
 Gundlach, B., Blum, J., Keller, H. U., & Skorov, Y. V. 2015, *A&A*, 583, A12
 Gundlach, B., Schmidt, K. P., Kreuzig, C., et al. 2018, *MNRAS*, 479, 1273
 Güttler, C., Mannel, T., Rotundi, A., et al. 2019, *A&A*, in press (arXiv:1902.10634)
 Hu, X., Shi, X., Sierks, H., et al. 2017, *MNRAS*, 469, S295
 Huizenga, D. G. 1984, Sci. Chem. Eng. Master thesis, Montana State Univ.
 Knudsen, M. 1928, *AnPh*, 285, 73
 Kührt, E., & Keller, H. U. 1994, *Icar*, 109, 121
 Lévasseur-Regourd, A.-C., Agarwal, J., Cottin, H., et al. 2018, *SSRv*, 214, 64
 Mannel, T., Bentley, M. S., Boakes, P. D., et al. 2019, *A&A*, in press
 Moreno, F., Muñoz, O., Gutierrez, P. J., et al. 2017, *MNRAS*, 469, S186
 Ott, T., Drolshagen, E., Koschny, D., et al. 2017, *MNRAS*, 469, S276
 Pajola, M., Lucchetti, A., Fulle, M., et al. 2017, *MNRAS*, 469, S636
 Rietmeijer, F. J. M. 1998, *Reviews in Mineralogy*, 36, 2
 Rotundi, A., Sierks, H., Della Corte, V., et al. 2015, *Sci*, 347, aaa3905
 Satterfield, C. N. 1970, *Mass Transfer in Heterogeneous Catalysis* (Cambridge, MA: MIT Press)
 Schulz, R., Hilchenbach, M., Langevin, Y., et al. 2015, *Natur*, 518, 216
 Skorov, Y. V., & Blum, J. 2012, *Icar*, 221, 1
 Smith, J. N. 1970, *Chemical Engineering Kinetics* (New York: McGraw-Hill)
 Tosi, F., Capaccioni, F., Capria, M. T., et al. 2019, *NatAs*, in press, <https://www.nature.com/articles/s41550-019-0740-0>
 Vincent, J.-B., A’Hearn, M. F., Lin, Z.-Y., et al. 2016, *MNRAS*, 462, S184